International Journal of Nanomedicine

Dovepress
open access to scientific and medical research

Open Access Full Text Article

ORIGINAL RESEARCH

Controlled release of chitosan/heparin nanoparticle-delivered VEGF enhances regeneration of decellularized tissue-engineered scaffolds

This article was published in the following Dove Press journal:
International Journal of Nanomedicine
30 April 2011
Number of times this article has been viewed

Qi Tan
Hao Tang
Jianguo Hu
Yerong Hu
Xinmin Zhou
Yunming Tao
Zhongshi Wu

Department of Cardiothoracic Surgery Second Xiangya Hospital, Central South University, Changsha 410011, People's Republic of China

Abstract: Regeneration deficiency is one of the main obstacles limiting the effectiveness of tissue-engineered scaffolds. To develop scaffolds that are capable of accelerating regeneration, we created a heparin/chitosan nanoparticle-immobilized decellularized bovine jugular vein scaffold to increase the loading capacity and allow for controlled release of vascular endothelial growth factor (VEGF). The vascularization of the scaffold was evaluated in vitro and in vivo. The functional nanoparticles were prepared by physical self-assembly with a diameter of 67–132 nm, positive charge, and a zeta potential of ~30 mV and then the nanoparticles were successfully immobilized to the nanofibers of scaffolds by ethylcarbodiimide hydrochloride/hydroxysulfosuccinimide modification. The scaffolds immobilized with heparin/chitosan nanoparticles exhibited highly effective localization and sustained release of VEGF for several weeks in vitro. This modified scaffold significantly stimulated endothelial cells' proliferation in vitro. Importantly, utilization of heparin/chitosan nanoparticles to localize VEGF significantly increased fibroblast infiltration, extracellular matrix production, and accelerated vascularization in mouse subcutaneous implantation model in vivo. This study provided a novel and promising system for accelerated regeneration of tissue-engineering scaffolds.

Keywords: nanoparticle, scaffolds, VEGF, control release, vascularization, regeneration

Introduction

Tissue-engineered scaffolds are the main substitute materials used to repair cardiovascular damage in cardiovascular diseases. However, poor integration of a tissue-engineered scaffold into the recipient's cardiovascular system and its incomplete regeneration, such as poor endothelialization and incomplete vascularization, limit the scaffold's clinical effectiveness. Poor endothelialization could induce thrombogenicity and calcification,[1] while incomplete vascularization could result in insufficient nutrient and oxygen supply to the scaffold.[2] Conventional cardiac tissue engineering can provide oxygen diffusion only at a distance of about 150 μm due to poor vascularization.[3,4] Therefore, complete regeneration would be a hallmark of a successful tissue-engineered scaffold.

We recently reported an in vivo application of decellularized scaffolds prepared from bovine jugular veins to reconstruct dog pulmonary and right ventricle with potential regeneration.[5–8] This decellularized scaffold is rich in important extracellular matrix proteins. In combination with photo-oxidative cross-linkage, decellularized bovine jugular veins were able to retain tensile strength, resist thrombosis, and exhibit

Correspondence: Zhongshi Wu
Department of Cardiothoracic Surgery, Second Xiangya Hospital, Central South University, Changsha, 410011, People's Republic of China
Tel +86 13974958180
Fax +86 073185292133
Email deepblue0630@yahoo.com.cn

potential for regeneration. However, the major problem is still the lack of cardiovascular integration and complete regeneration.

Regeneration of scaffolds requires formation of new blood vessels to supply both nutrients and oxygen. Angiogenic processes are regulated by various growth factors. Vascular endothelial growth factor (VEGF) is one of the most important and widely studied growth factors, and has been shown to be useful for enhancing regeneration of scaffolds.[6] However, excessive amounts of VEGF are required because of its short half-life (~50 minutes). This is usually accomplished by the administration of high doses of VEGF, which can induce severe side effects, such as undesired vascularization at nontarget sites, tumor growth at locations away from the scaffold, hypotension, and edema.[9,10] In contrast, sustained local concentration of growth factors is necessary for the development of mature blood vessels. Therefore, it is particularly important to localize VEGF to the scaffold and control its release at the site of implantation.

A number of growth factors and other bioactive molecules possess conserved amino acid sequences which could be the heparin-binding sites.[11,12] Based on the specificity of factors for heparin, several heparin-containing systems have been developed for controlled release of growth factors.[13–16] Among these the direct immobilization of heparin onto the scaffold surface, and subsequent attachment of growth factors, is currently the most popular strategy for local delivery of growth factors. For instance, VEGF can be covalently bound to activated collagen scaffolds by cross-linking agents.[16] After attachment to heparinized acelluar collagen, VEGF can increase endothelial cell proliferation,[17] upregulate microvasculature formation, and stimulate blood vessel maturation.[18–20] Polymeric matrices have also been successfully used to deliver angiogenic proteins to scaffolds and sustained release was established. These include dextran hydrogels,[21] alginate hydrogels,[22] alginate beads,[23] hyaluronan hydrogels,[24] and poly(DL-lactic-co-glycolic acid scaffolds.[25] Recently, drug delivery of VEGF via heparin-functionalized nanoparticles/fibrin complex revealed efficient revascularization.[10] However, there are many drawbacks that still hamper the clinical application of these engineered scaffolds. These drawbacks include rapid release and clearance of growth factors, the large dose of encapsulated proteins that is required, reduced growth factor bioactivity by chemical modification, denaturation of the growth factor due to residual cross-linkers, and complications in the host caused by systemic administration of nanoparticles. Therefore, a larger loading-capacity, sustained biological activity and local delivery as well as controlled release of growth factors are the key factors for the effective application of decellularized tissue-engineered scaffolds in a clinical setting.

Chitosan is a natural, biocompatible, and biodegradable cationic polysaccharide the applications of which in tissue engineering and drug delivery have been widely studied. The accumulated evidence demonstrated that chitosan could stimulate cell attachment and growth.[26,27] Heparin is a negatively charged, linear polysaccharide present in many living organisms and a member of the glycosaminoglycan superfamily.[28] The physical adsorption of heparin could prevent early degradation of growth factors, thereby preserving their biological activity. With its capacity for antithromobogenicity, heparin is used for suppressing acute subthrombus.[29–31] Thus, a chitosan and heparin nanoparticle provides a large loading capacity while stimulating regeneration and preventing early degredation.[28]

In this study, our main objective is to develop a scaffold with large loading capacity, retention of biological activity, and a sustained local release of VEGF to enhance the vascularization of decellularized bovine jugular vein scaffolds. The large loading capacity was established by the application of nanoparticles to localize VEGF. To preserve the biological activity, functional heparin/chitosan nanoparticles were prepared via physical self-assembly without residual cross-linkers. Local delivery and controlled release of VEGF was established by ethylcarbodiimide hydrochloride/hydroxysulfosuccinimide modification of heparin/chitosan nanoparticles and subsequent attachment to scaffolds. This system exhibited a significant enhancement of regeneration in bovine jugular vein scaffolds.

Materials and methods

Materials

1-(3-Dimethylaminopropyl)-3-ethylcarbodiimide hydrochloride (EDC, Sigma-Aldrich, St. Louis, MO) and N-hydroxysulfosuccinimide (NHS, Pierce Chemicals, Dallas, TX) were used to chemically modify nanoparticles and subsequently attach them to scaffolds. 2-(4-morpholino)ethanesulfonic acid hydrate (MES, Sigma-Aldrich) was used as a buffer during EDC/NHS modification of nanoparticles and subsequent attachment to scaffolds. 3-(4,5-dimethylthiazol-2-yl)2,5-diphenyltetrazolium bromide (MTT, Sigma-Aldrich) was used for cell proliferation assay. Human recombinant VEGF-165 was purchased from Cell Signaling technology (Danvers, MA). Fluorescein diacetate (FDA) and Dulbecco's Modified Eagle's Medium (DMEM) were purchased from Invitrogen Inc. (Carlsbad, CA).

Preparation of decellularized and photo oxidized scafffolds

The bovine jugular veins (BJV) of buffaloes (300 to 500 kg) were obtained from the local slaughterhouse. The scaffolds were prepared from BJV by multistep detergent-enzymatic decellularization and dye-mediated photo-oxidation procedures (DP) as previously described.[7] The DP scaffolds were the unmodified scaffolds for nanoparticle loading, modification, and VEGF localization in this study.

Preparation of functional heparin/chitosan nanoparticles

Low-molecular-weight chitosan was obtained by a depolymerization method.[32] Heparin/chitosan nanoparticles were prepared by physical self-assembly method. Briefly, an aqueous solution of chitosan (pH 5.0, 2 mL) was combined with aqueous heparin (5 mL) at various mass ratios and then magnetically stirred for 15 minutes at 30°C. The aggregates were removed by passing the solution through a 0.2 μm filter. Free heparin and chitosan were removed by washing the nanoparticles 3 times with distilled water and then the nanoparticles were collected by centrifugation at 14,000 rpm for 15 minutes in a bench-top centrifuge.

Particle size, distribution, and zeta potential of heparin/chitosan nanoparticles were measured by laser diffraction Mastersizer (Malvern Instruments, UK). The morphology of nanoparticles was examined by environmental scanning electron microscope (SEM, JEOL, Tokyo, Japan). The loading efficiency and loading content of heparin in tested nanoparticles were determined by the amount of free heparin left in the supernatant using a colorimetric method and calculated as previously described.[33]

$$\text{Loading efficiency} = (\text{total amount of heparin added} - \text{free heparin})/\text{total amount of heparin added} \times 100\%.$$

$$\text{Loading content} = (\text{total amount of heparin added} - \text{free heparin})/\text{weight of nanoparticles} \times 100\%.$$

Immobilization of heparin/chitosan nanoparticles to scaffolds and then localizing VEGF-165

To prepare the immobilization buffer, EDC and NHS were dissolved in 2-(4-morpholino) ethanesulfonic acid hydrate (MES) buffer at a concentration of 6 mg/mL and 3.6 mg/mL, respectively. The MES buffer was prepared by dissolving MES in dH_2O (1.06% [W/V], pH 5.5). Scaffolds (10×10 mm^2 in area and 5 mm in thickness) were cut from the conduit of DP. The scaffolds (SF) were placed in 5 mg/mL of nanoparticle (NP) solution for 4 hours, and then washed with fresh phosphate buffer saline (PBS) for 5×5 minutes. The nanoparticle-treated scaffolds were then immersed in 1 mL of immobilization buffer and continuously incubated for 4 hours at 37°C, followed by washing with PBS for 5×5 minutes to produce SF-NP (with EDC/NHS). The control scaffolds included: 1) unmodified scaffolds (SF-DP); 2) SF-NP incubated with PBS and without EDC/NHS (SF-NP no EDC/NHS).

To localize VEGF-165, scaffolds (SF-NP with EDC/NHS, SF-NP without EDC/NHS treatments) were immersed in 1 mL of PBS containing 43, 113, or 237 ng/mL of VEGF overnight at room temperature. After reaction, the scaffolds were washed 5 times with fresh PBS, and then collected after removing free VEGF. The amount of VEGF remaining in the VEGF immersion solution and the PBS washing solution was determined by ELISA using the Quantikine human VEGF ELISA kit (RandD Systems). A standard curve ranging from 62.5 to 1000 pg/mL was determined by using the standard VEGF-165 protein provided with the ELISA kit. To quantify the physical adsorption of VEGF to scaffolds, 43, 113, or 237 ng/mL of VEGF were incubated with the SF-DP (SF-DP-VEGF) and free VEGF was measured.

Characteristics of SF-NP-VEGF

The scaffolds immobilized with nanoparticles and localized with VEGF (SF-NP-VEGF) were imaged by environmental scanning electron microscopy (SEM, Hitachi S-3400N, Japan). Surface roughness was determined by atomic force microscopy (AFM) (Nanoscope III, Digital Instruments, Santa Barbara, CA).

Quantification of VEGF release in vitro

The amount of VEGF released from SF-NP-VEGF treated with or without EDC/NHS (n = 3) was assessed using a commercially available ELISA kit (RandD Systems). Briefly, scaffolds were immersed in 1 mL of release buffer (0.1% bovine serum albumin in PBS [pH 7.2]). The release buffer was replaced at designed time intervals from 0 to 30 days and frozen at –20°C until the analysis. Concentrations of VEGF determined from a standard curve ranged from 62.5 to 1000 pg/mL.

EA.hy926 cells, derived from human umbilical vein endothelial cells, were acquired originally from the American Type Culture Collection (ATCC, Cat#: CRL-2922) and cultured in DMEM medium containing 10% fetal bovine serum. The scaffolds (SF-NP) loaded with 50 ng/mL, or

250 ng/mL of VEGF, were incubated in a 24-well plate for 60 minutes before seeding cells. The SF-DP was used as a control. A total of 5×10^4 cells in 10 µL medium was seeded onto each scaffold for 1 hour at 37°C, followed by addition of 1 mL of fresh culture medium. Cells were continually cultured for 1, 3, or 7 days.

Live imaging of cell morphology on scaffolds

To visualize cell morphology, scaffolds seeded with EA.hy926 cells were imaged under confocal laser scanning microscopy (Leica TCS-NT) after staining with FDA. The seeded scaffolds were rinsed in PBS containing FDA (5 mM) at 37°C for 10 minutes, and finally observed under confocal laser scanning microscopy.

MTT assay

To determine the viability of cultured endothelial cells, scaffolds (SF-DP, SF-NP, SF-NP treated with 50 ng/mL or 250 ng/mL of VEGF) were prepared as described above. MTT was dissolved in PBS at 5 mg/mL. Twenty microliters of the MTT solution was added to each well, and the plates were incubated at 37°C for 4 hours. After removing the medium, 150 µL of DMSO was added to each well. After gently shaking for 10 minutes, the absorbance was read at a wavelength of 570 nm in a plate reader.

Angiogenesis and regeneration potential in mice

To evaluate regeneration of scaffolds, SF-DP or SF-NP-VEGF was implanted into the subcutaneous pockets of 8-week-old male BALB/c mice (Chinese Academy of Medical Sciences). All mice were given free access to food and water in accordance with an approved protocol from the South Central University. Mice were anesthetized by intraperitoneal injection of chloral hydrate. The dorsal hair coat was clipped, disinfected with betadine and alcohol, and a 12-mm dorsal midline incision was made. One subcutaneous pocket on each side was prepared, and 1 scaffold was inserted into each pocket. The incision was then closed with interrupted prolene sutures. Each mouse received 2 implants of the same composition, and 6 mice were assigned to each group. Four and 8 weeks post surgery, the mice were sacrificed and tissue sections were prepared from the implants.

Histological characteristics

Formalin-fixed, paraffin-embedded sections were stained with hematoxylin and eosin (H&E) to evaluate cell infiltration and capillary density. The capillaries were counted under light microscopy. The density of capillary per mm^2 was calculated by the total amount of capillaries in 10 random areas of 1 mm^2/10. The endothelial cells were further identified by anti-CD31 antibody (Bioss Biological Technology Ltd., China). The primary myelofibrosis was detected by Herovici staining.[34] Scott's alcian blue method was used to detect glycosaminoglycans.[35] Macrophages were detected by CD68 antibody (clone MAC 387, Lab Vision Corp.) as previously described.[36] Fibroblasts were characterized by the presence of vimentin antigen and stained with polyclonal rabbit antibody (Bioss Biological Technology Ltd., China) by following the established protocol.[37]

Briefly, the postoperative scaffolds were fixed with 10% formalin overnight at 4°C. After they were washed with PBS, the scaffolds were embedded in paraffin and cut into 5-µm sections. After deparaffinization and rehydration, the scaffold sections underwent antigen retrieval with citric acid solution (Maixin Biological Technology Ltd, CA) in a pressure cooker for 3 minutes. The sections were then incubated with peroxidase inhibitor (3% H_2O_2) in the dark for 15 minutes, and nonspecific sites were blocked by 10% goat serum for 30 minutes at room temperature. Sections were then incubated with primary antibody for 1 hour at room temperature. Slides were washed twice with PBS, and secondary antibody (Super Sensitive Detection System; Maixin) was then applied. After slides were washed with PBS again, they were developed with diaminobenzidine Chromogen (Maixin) for 15 minutes. Slides were washed with water, counterstained with Gill's hematoxylin and placed in 0.5% ammonium hydroxide.

Statistical analysis

The experimental values are expressed as mean ± SEM. Comparisons between the two groups were performed with a 2-tailed *t* test for unpaired data. A $P < 0.05$ was considered to be statistically significant.

Results

Characteristics of heparin/chitosan nanoparticles

Table 1 shows the particle size, polydispersity (PDI), and zeta potential of nanoparticles which were prepared at various concentrations of chitosan and heparin with a ratio of 5:2 in mass (pH 4.5). Table 2 shows the particle size, PDI, and zeta potential of nanoparticles which were prepared at pH 4 to 6 of chitosan (1 mg/mL) and heparin (2 mg/mL). The particle size of the nanoparticles varied from 67 to 132 nm and their zeta potential values were positive or negative.

Table 1 The effect of concentration on the characteristics of Heparin/Chitosan nanoparticles

Heparin conc (mg/mL)	Chitosan conc (mg/mL)	Particle size (nm)	Polydispersity	Zeta potential (mv)
0.5	1	72.1 ± 7.3	0.117 ± 0.008	28.5 ± 1.2
1	2	87.6 ± 6.2	0.157 ± 0.011	29.2 ± 1.7
1.5	3	98.8 ± 8.7	0.192 ± 0.013	30.1 ± 1.5
3	1.5	83.6 ± 2.3	0.087 ± 0.005	−14.6 ± 3.9
2	1	79.2 ± 6.1	0.056 ± 0.003	−19.1 ± 2.1
1	0.5	70.1 ± 5.7	0.135 ± 0.068	−23.8 ± 5.1

Notes: heparin/chitosan = 2/5; n = 4.

The PDI measures the homogeneity with ranges from 0 to 1. A higher PDI indicates a higher heterogeneity. In this study, nanoparticles were chosen with positive charge, about 30 mV zeta potential, and a PDI of 0.086 ± 0.007.

We found that the loading efficiency of nanoparticles prepared by 2 mg/mL of chitosan with 1 mg/mL of heparin or 1 mg/mL of chitosan with 0.5 mg/mL of heparin with a 4:1 mass ratio (chitosan:heparin) was highest and no differences were observed between the two preparations (93.2% ± 1.43%, $P > 0.05$). However, the loading content of nanoparticles prepared at 2 mg/mL of chitosan with 1 mg/mL of heparin (0.68 ± 0.17 mg/mg) was greater than that of nanoparticles prepared at 1 mg/mL of chitosan with 0.5 mg/mL of heparin (0.43 ± 0.06 mg/mg). Therefore, the nanoparticles prepared with the former formulation were chosen for the subsequent studies.

Porous structure of scaffolds with immobilized nanoparticles and localized VEGF

The morphology of scaffolds was observed under environmental SEM. The SF-DP exhibited nanofiber characteristics, such as 3-dimensional structure, high porosity, and high surface-to-volume ratio. The microporous structure of SF-DP consisted of interconnected pores with an average diameter of 120 nm and an average wall thickness of 230 nm.

Table 2 The effect of pH value on the characteristics of Heparin/Chitosan nanoparticles

Heparin pH	Particle size (nm)	Polydispersity	Zeta potential (mV)
4	68.3 ± 3.4	0.090 ± 0.018	26.1 ± 2.6
4.5	75.1 ± 3.1	0.135 ± 0.068	27.1 ± 1.1
5	103.0 ± 6.2	0.176 ± 0.074	29.1 ± 1.7
5.5	238.2 ± 12.3	0.290 ± 0.087	29.4 ± 0.8
6	876.6 ± 52.8	0.610 ± 0.110	29.2 ± 3.1

Notes: Heparin = 1 mg/mL; Chitosan = 2 mg/mL; n = 4.

Pores 450 nm in diameter and fibers 1.2 μm diameter were also observed (Figure 1A and B). The SF-NP exhibited sheaths enclosed within a bundle of nanofibers (Figure 1C and D). Surface roughness was determined by AFM. As shown in Figure 1E and F, the SF-NP has a smoother surface (RMS = 67.34 nm), while SF-DP had a rougher surface (RMS = 137.83 nm) (Figure 1E and F).

Scaffolds immobilized with nanoparticles loaded more VEGF

VEGF could be localized to nanoparticles abundantly and stably through physical adsorption and modification of scaffolds. As shown in Figure 2A, VEGF was loaded in a concentration-dependent manner. The SF-NPs with EDC/NHS treatment exhibited significantly greater efficiency ($P < 0.01$) in loading VEGF compared with SF-NP without EDC/NHS treatment and SF-DP at graded concentrations of VEGF (Figure 2A). Interestingly, SF-DP loaded 43 ± 8 ng of VEGF, possibly because the chondroitin sulfate in extracellular matrix was able to attach to VEGF.

Controlled release of VEGF

The release of VEGF from nanoparticles immobilized to scaffolds was analyzed over a period of 30 days (Figure 2B). VEGF was released with a high burst (62% to 70%) during the first 3 days and 86% to 93% of the total VEGF was released at 7 days from SF-NP-VEGF without EDC modification (physical adsorption). In contrast, VEGF was released with a significantly reduced burst from SF-NP-VEGF with EDC modification (physical adsorption plus EDC modification). The lower concentration group (50 ng/mL) released ~37.12% at 30 days and the higher concentration group (250 ng/mL) released 42.17% at 30 days. In the EDC-modified SF-NP-VEGF, VEGF localized by massive nanoparticles still existed on the surface of scaffolds while some nanoparticles had swelled to a large diameter at 4 and 10 weeks (Figure 2C and D).

Effect of nanoparticle-localized VEGF on endothelial cell proliferation in vitro

To test whether our SF-NP-VEGF could promote vascularization in decellularized scaffolds, we performed MTT assay to measure the viability and proliferation of endothelial cells on scaffolds. As shown in Figure 3A, SF-NP-VEGF, loaded with 50 ng/mL or 250 ng/mL of VEGF induced clear increases in the proliferation of endothelial cells at day 3 and day 7 compared with SF-DP. This result suggests that VEGF localized by nanoparticles promoted the endothelial

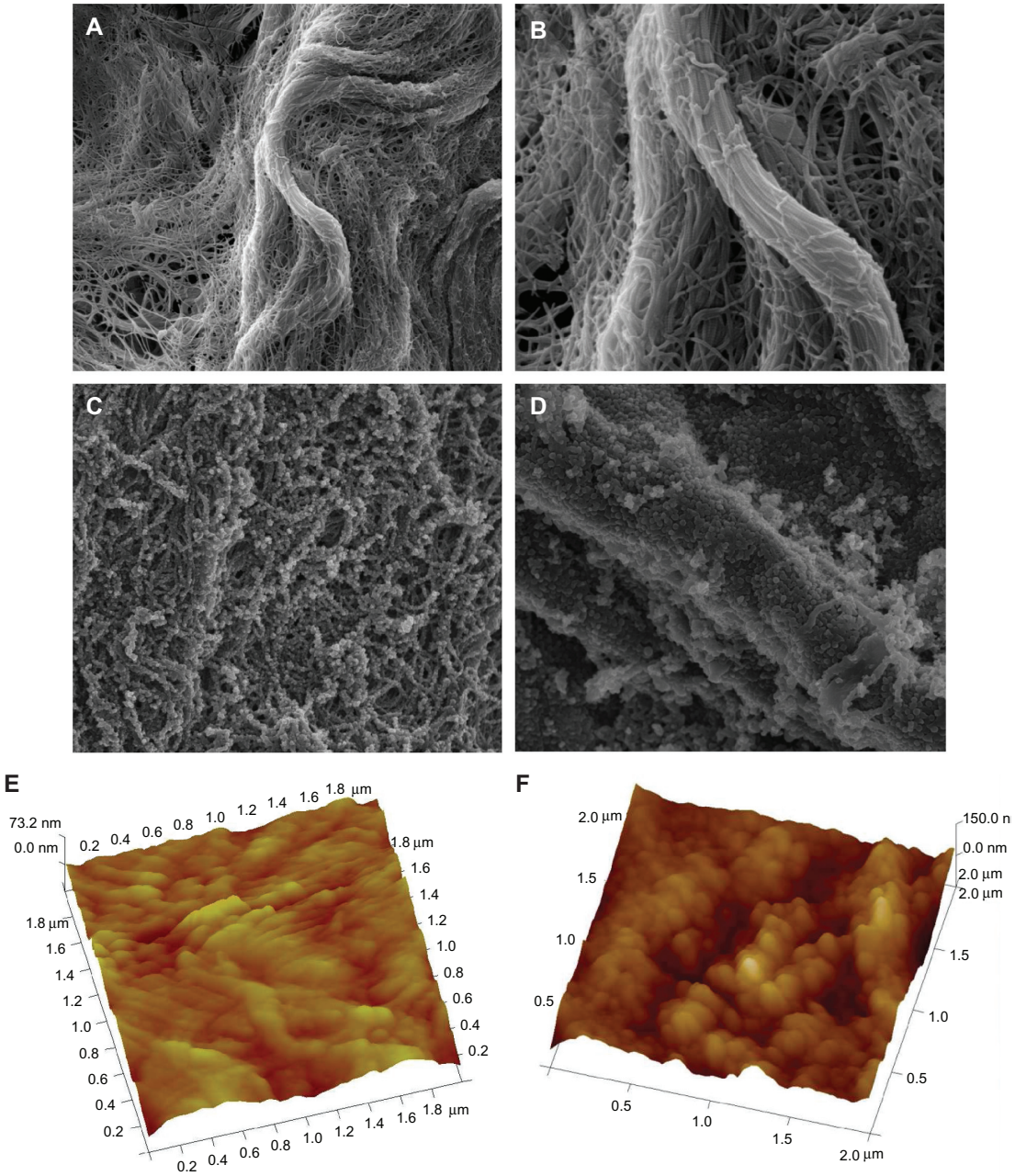

Figure 1 The morphology of scaffolds. **A**) Morphology of photo-oxidative cross-linked decellularized scaffolds (SF-DP) from bovine jugular vein (BJV), magnification × 10,000. **B**) Morphology of SF-DP, magnification × 30,000. **C**) Morphology of heparin/chitosan (HEP/CS) nanoparticle-immobilized scaffold (SF-NP), magnification × 10,000. **D**) Morphology of HEP/CS nanoparticle-immobilized scaffold (SF-NP), magnification × 30,000. **E**) Surface roughness of SF-DP determined by atomic force microscopy (AFM). **F**) Surface roughness of SF-NP determined by AFM.

cell proliferation on the surface of scaffolds. To minimize the influence of affinity for different scaffolds, we performed MTT assay 8 hours after cell seeding and found no significant differences between SF-NP-VEGF (50 or 250 ng/mL of VEGF) and SF-DP (data not shown).

We further observed the morphological changes of endothelial cells. As expected, SF-NP-VEGF exhibited more elongated endothelial cells on the surface of scaffolds at day 3 and day 7 of the incubation compared with unmodified scaffolds (SF-DP). Importantly, FDA staining showed significantly more circular structures in endothelial cells in the SF-NP-VEGF group compared with the SF-DP group (Figure 3B). These circular structures might suggest cell organization and vascularization, rather than cell aggregation alone.

Histological evidence of regeneration

Regeneration of scaffolds was further analyzed by subcutaneous implantation of EDC-modified SF-NP-VEGF scaf-

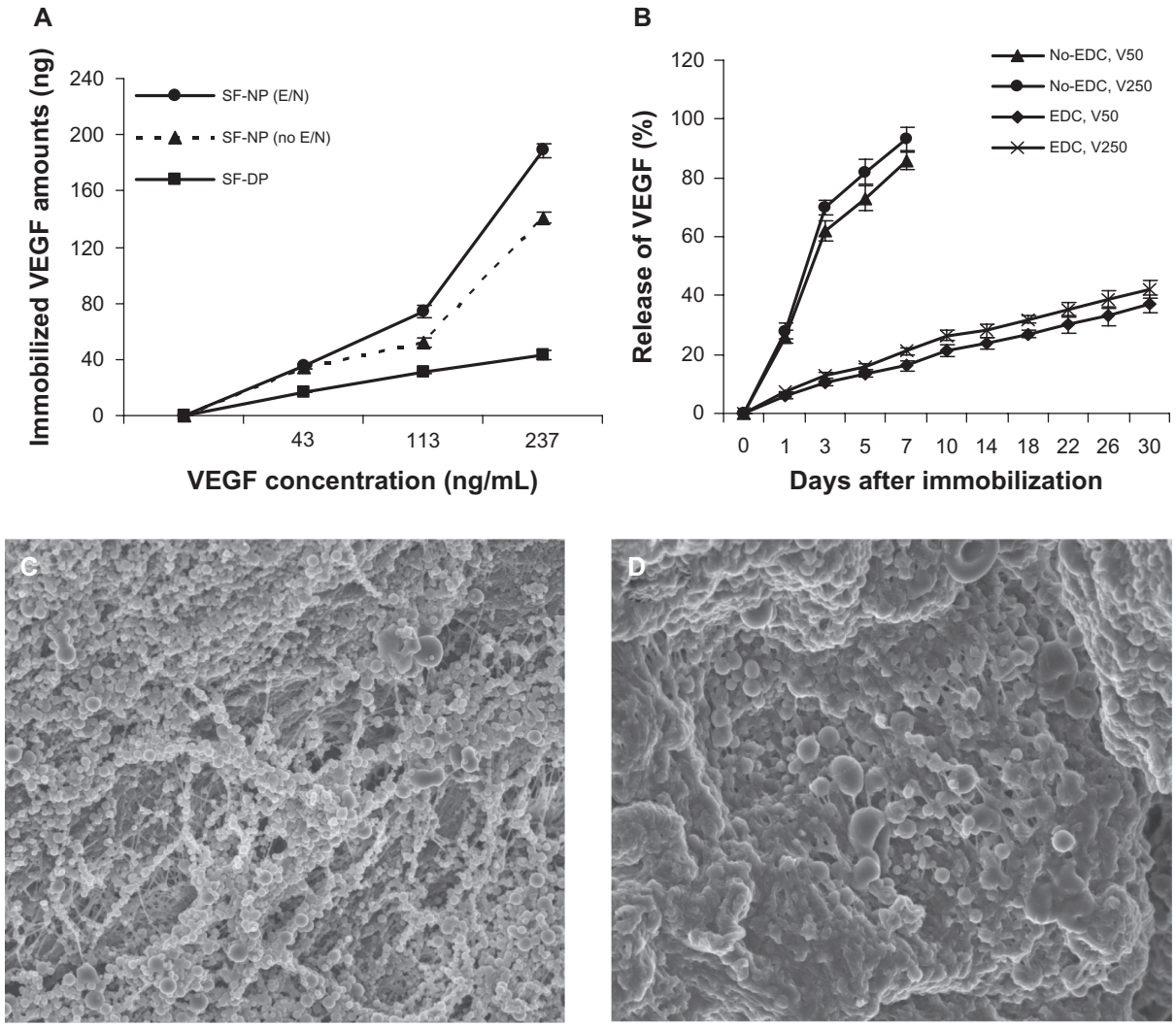

Figure 2 The characteristics of nanoparticle (NP)-delivered vascular endothelial growth factor (VEGF). **A**) Entrapping of VEGF in a concentration-dependent manner. **B**) Controlled release of VEGF from NPs localized at scaffolds. In the EDC-modified SF-NP, massive NPs entrapping VEGF still existed on the surface of scaffolds 4 weeks (**C**) and 10 weeks (**D**).

Abbreviations: EDC, 1-(3-Dimethylaminopropyl)-3-ethylcarbodiimide hydrochloride; DP, decellularized scaffolds; SF, scaffolds; V/VEGF, vascular endothelial growth factor

folds in mice. Encouragingly, new vessels were easily seen in SF-NP-VEGF scaffolds at 4 weeks and 8 weeks after implantation while fewer new vessels were seen in SF-DP scaffolds (Figure 4). H&E staining also showed new capillaries in repopulated layers and tissues surrounding the implanted SF-NP-VEGF scaffolds, whereas almost no noticeable capillaries were observed in SF-DP scaffolds at 4 weeks. Eight weeks after implantation, SF-NP-VEGF scaffolds showed significantly more new capillaries than SF-DP (Figure 5A). The difference in capillary density (the number of capillaries per mm^2) between SF-NP-VEGF (132 ± 26 for 250 ng/mL VEGF, 118 ± 19 for 50 ng/mL VEGF) and SF-DP (39 ± 8) was statistically significant ($P < 0.001$, $n = 8$) (Figure 5B). The significant vascularization in the SF-NP-VEGF implantation was further verified by CD31staining (Figure 6). Thus, the angiogenic bioactivity of nanoparticle-localized VEGF was evident in vivo.

The migration of host cells into the scaffolds was analyzed by the infiltration of host cells into scaffolds. In the SF-NP-VEGF (250 ng/mL) implant, host cells were homogenously distributed into one-fourth of the outer surface of scaffolds at 4 weeks and three-fourths at 8 weeks (Figure 5). This suggests that the migration process began at the adventitia and proceeded continuously towards the luminal surface. In the SF-DP implant, distribution of host cells was observed at only one-tenth of the outer surface of scaffolds at 4 weeks and one-fourth at 8 weeks.

Generally, surface collagen cross-linkage could reduce immunological response, but it also blocks cellular infiltration. We further verified that the main infiltrated cells

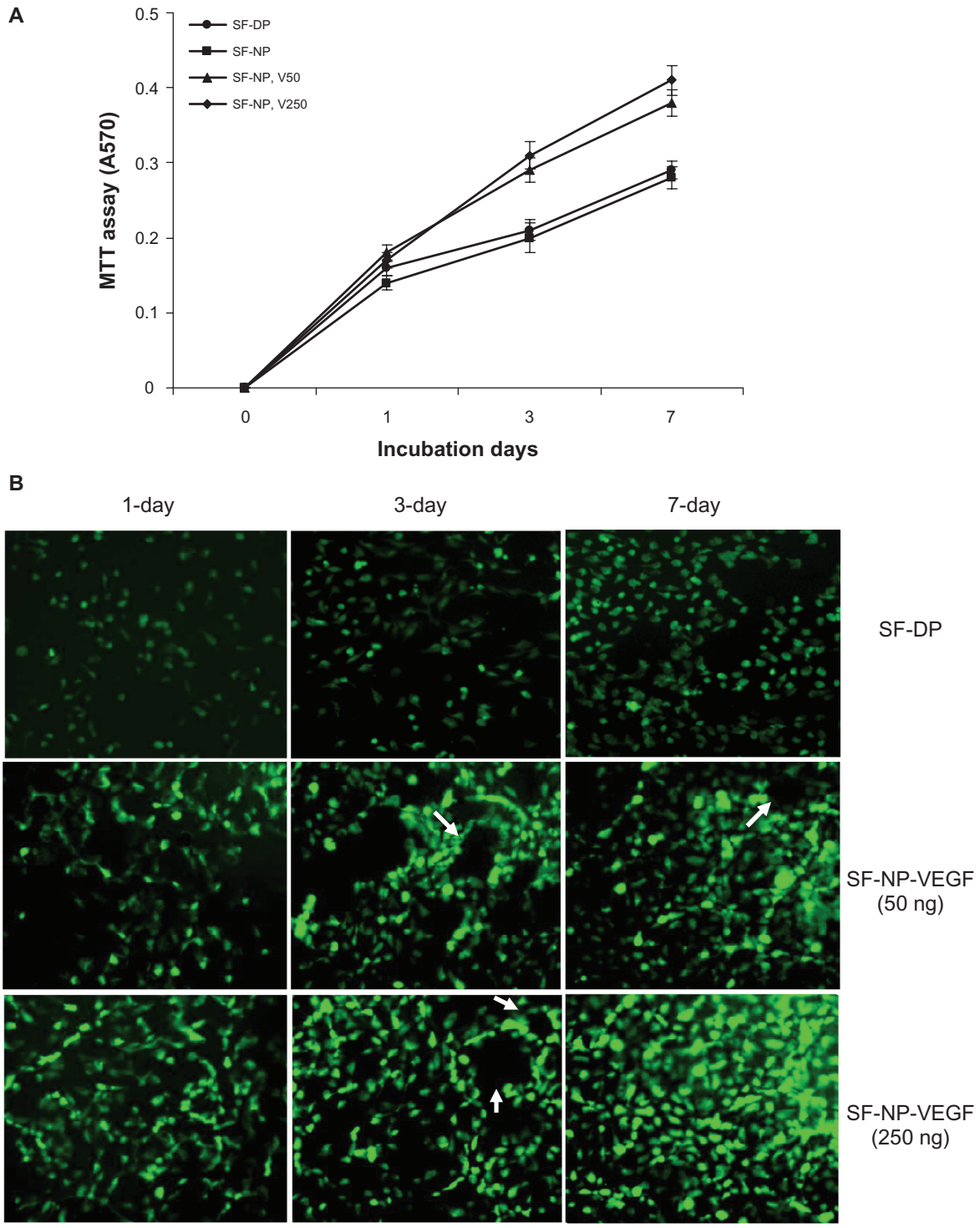

Figure 3 Nanoparticle-delivered VEGF stimulates endothelial cell proliferation and tube formation. **A**) MTT assay of the viability and proliferation of endothelial cell (EC) on scaffolds. **B**) Morphological changes of EC at 2, 3, or 7 days after incubation. SF-NP-VEGF showed more elongated EC cells and circular structures (tube formation) at day 3 and day 7.

Abbreviations: DP, decellularized scaffolds; MTT, 3-(4,5-dimethylthiazol-2-yl)2,5-diphenyltetrazolium bromide; NP, nanoparticles; SF, scaffolds; V/VEGF, vascular endothelial growth factor

were fibroblasts (the vimentin positive cells) (Figure 7) and only a few macrophages (Figure 8) were seen at 8 weeks post implantation.

Figure 9 shows staining for extracellular matrix components of scaffolds at 4 and 8 weeks post implantation. Herovici staining showed the red mature collagen fibrils in all layers, but SF-NP-VEGF showed more new collagen fibrils (blue) (Figure 9B and C). Scott's alcian blue staining showed that glycosaminoglycans were present in all layers of the wall (Figure 10). In the SF-NP-VEGF implant, blue newly

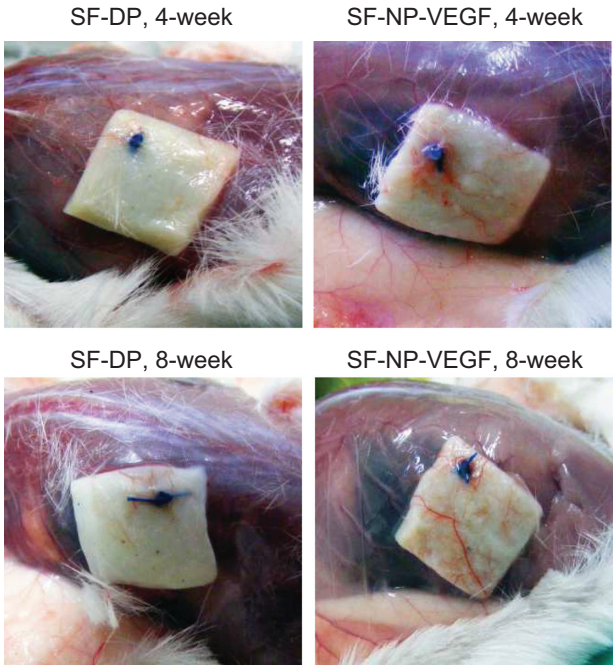

Figure 4 New vessel formation in SF-NP-VEGF implants. More new vessels were clearly seen in SF-NP-VEGF scaffolds at 4 weeks and 8 weeks after implantation.
Abbreviations: DP, decellularized scaffolds; NP, nanoparticle; SF, scaffolds; VEGF, vascular endothelial growth factor

synthesized collagen fibrils were produced by fibroblasts and covered one-sixth of regions near the outer layer at 4 weeks. The glycosaminoglycans were present in the outer layer regions in accordance with newly synthesized collagen fibrils, as well as the areas of the host cell repopulation. At 8 weeks, the newly synthesized collagen fibrils (Figure 9) and glycosaminoglycans (Figure 10) were distributed on half of the walls of the scaffold. In the SF-DP group, newly synthesized collagen fibrils and glycosaminoglycans covered less than one-fourth of the surface area. This suggests that SF-NP-VEGF could accelerate cell infiltration and tissue remolding.

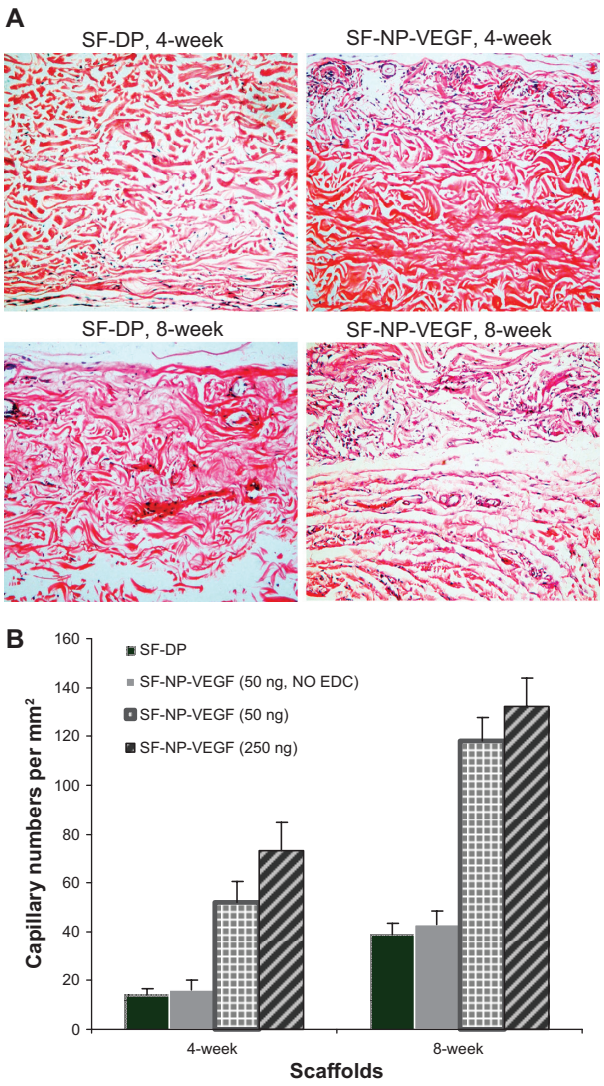

Figure 5 H&E staining of implant sections and capillary density. **A**) H&E staining showed new capillaries in repopulated layer and tissues surrounding the implants at 4 and 8 weeks, original magnification × 200. **B**) The capillary density calculated as the number of capillaries per mm^2.
Notes: N = 8; $P < 0.001$.
Abbreviations: H&E, hematoxylin and eosin; DP, decellularized scaffolds; NP, nanoparticle; SF, scaffolds; VEGF, vascular endothelial growth factor

Discussion

Optimal tissue-engineered cardiovascular structures should be fully biocompatibile and capable of complete regeneration. In our previous study, decellularized BJV scaffolds were used to reconstruct sections of pulmonary arteries and right ventricles in a dog. This invention provided a preliminary view that the acellular BJV scaffolds could resist thrombosis and calcification with good regeneration potential and excellent hemodynamic performance.[5–8] In spite of the progress with this scaffold, there are still some issues, such as the delayed regeneration and insufficient revascularization, which still needed to be resolved. In this study we created a heparin/chitosan nanoparticle, which can be effectively immobilized to the decellularized BJV scaffolds. The nanoparticle-immobilized scaffolds exhibited a high loading capacity and controlled release for VEGF which enhanced vascularization of the scaffold in vitro and in vivo.

In this study we prepared heparin/chitosan nanoparticles by self-assembly. Interestingly, their zeta potential values were either positive or negative. The positive or negative charges might be determined by the relative ratios of the surface molecules (chitosan or heparin), whichever is more dominant (Table 1). Most heparin/chitosan nanoparticles exhibited positive charges because they were covered with more chitosan than heparin. However, we hypothesized that nanoparticles with higher ratios of heparin to chitosan on the surface will exhibit a nega-

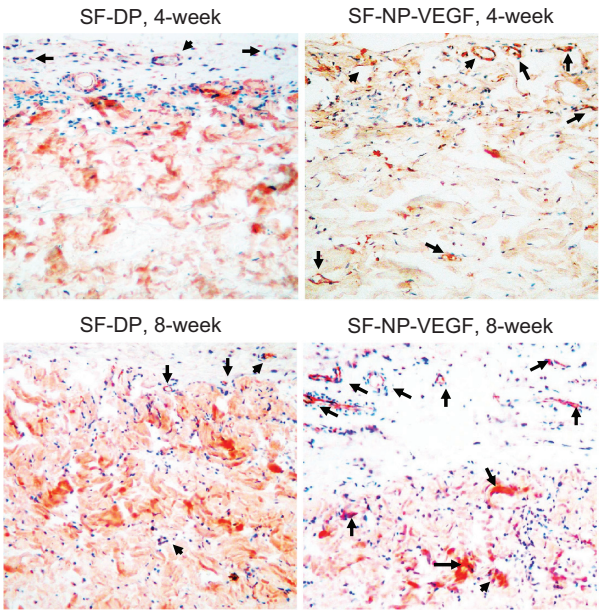

Figure 6 CD31staining of implant sections. The endothelial cells were stained by anti-CD31 antibody, original magnification × 200.
Note: The arrows indicate the positive staining.
Abbreviations: CD31, cluster of differentiation molecule 31; DP, decellularized scaffolds; NP, nanoparticle; SF, scaffolds; VEGF, vascular endothelial growth factor

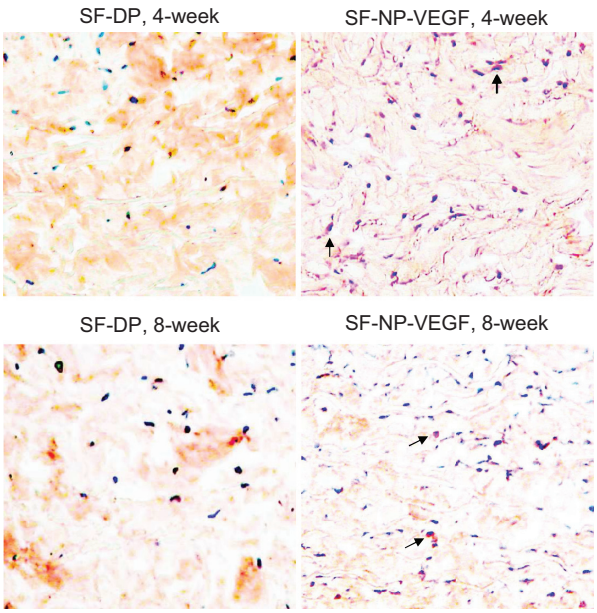

Figure 8 Immunohistochemical staining of macrophages. The macrophages were stained by anti-CD68 antibody, original magnification × 100.
Note: The arrows indicated red staining cells are macrophages.
Abbreviations: CD68, cluster of differentiation molecule 68; DP, decellularized scaffolds; NP, nanoparticle; SF, scaffolds; VEGF, vascular endothelial growth factor

tive charge and could bind more VEGF. Unexpectedly, the primary experiment revealed that nanoparticles with negative charges were unevenly distributed throughout the surface of the scaffolds. In contrast, nanoparticles with positive charge and a zeta potential of ~30 mV and a relatively uniform size <0.10 (PDI) were more efficient in immobilizing to the surface of scaffolds and localizing VEGF. This might be because the main components of the decellularized tissue-engineered scaffolds are collagen fibers, which are negatively charged under physiological conditions. Thus, nanoparticles with positive charges can effectively bind to the scaffolds. We also found that the

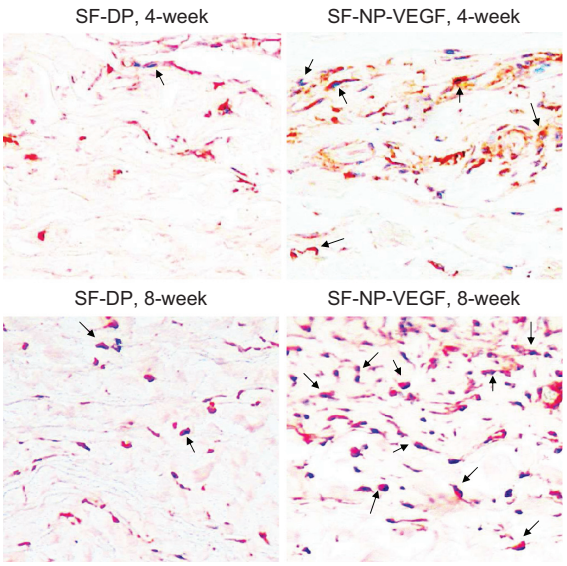

Figure 7 Immunohistochemical staining of fibroblasts. The fibroblasts were stained by anti-vimentin antibody, original magnification × 200. The red stained cells are the fibroblasts.
Note: The arrows indicate positive staining.
Abbreviations: DP, decellularized scaffolds; NP, nanoparticle; SF, scaffolds; VEGF, vascular endothelial growth factor

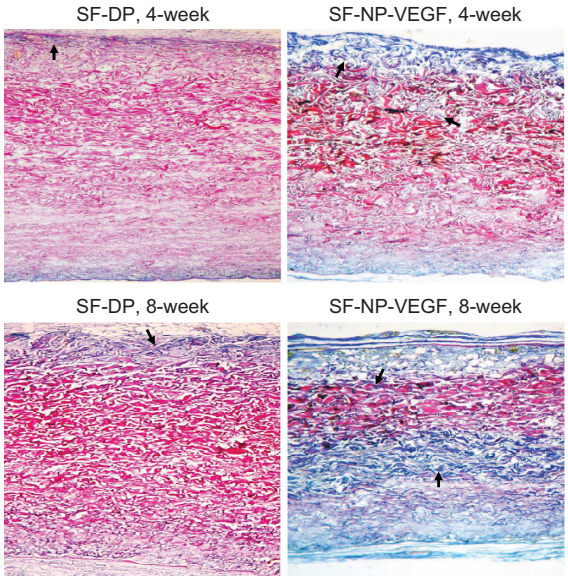

Figure 9 Herovici staining of collagen fibrils. Staining showed extracellular matrix components of scaffolds at 4 and 8 weeks implantation, original magnification × 200.
Notes: Red indicates the mature collagen fibrils and blue indicates new collagen fibrils. The arrows indicate positive staining of new collagen fibrils.
Abbreviations: DP, decellularized scaffolds; NP, nanoparticle; SF, scaffolds; VEGF, vascular endothelial growth factor

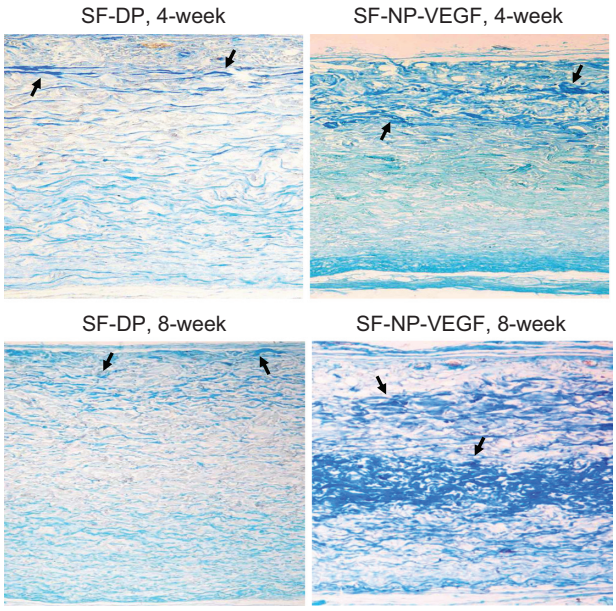

Figure 10 Glycosaminoglycans (GAG) staining. Scott's alcian blue staining showed that GAGs were present in all layers of the wall, original magnification × 100. More blue staining (new collagen fibrils) was observed in SF-NP-VEGF implant at 4 and 8 week.
Note: The arrows indicate positive staining of new collagen fibrils.
Abbreviations: DP, decellularized scaffolds; NP, nanoparticle; SF, scaffolds; VEGF, vascular endothelial growth factor

loading efficiency of nanoparticles exhibited no significant difference between different preparations, possibly because the amount of chitosan used (positive charge) significantly exceeded the amount of heparin (negative charge). Therefore, almost all of heparin molecules were cross-linked with chitosan into the complexes and yielded a high loading efficiency. The optimal size of nanoparticles designed for drug delivery is approximately 50 to 150 nm, which confers a high surface area-to-volume ratio. In this study, the particle size of the heparin/chitosan nanoparticles varied from 67 to 132 nm, suggesting an ideal size for drug delivery.

The heparin/chitosan nanoparticles were immobilized to the natural nanofiber of scaffolds through chemical modification. The microporous structure of scaffolds consisted of interconnected pores with an average diameter of 120 nm (Figure 1). Therefore, nanoparticles (67 to 132 nm in size) could not only cover the surface of scaffolds, but also penetrate deep into the matrix through interspaces. This is why a smoother surface was observed in nanoparticle-bound scaffolds (SF-NP) (Figure 1). Previous studies demonstrated that EDC can reinforce the nanoparticle's structure.[38,39] Therefore, chemical modification might also make the scaffold smooth and tight, which should be suitable for the endothelial cell attachment and proliferation. Among the big family of vascular endothelial growth factors, isoforms 165, 169, and 206 (VEGF-165, -169, -206) bind heparin with the greatest affinity. However, VEGF-169 and VEGF-206 can diffuse into the extracellular matrix and affect the cellular uptake due to their excessive affinity. In contrast, VEGF-165 is a better candidate for the study of controlled local release because of relatively lower affinity and effective revascularization. Importantly, after the heparin/chitosan nanoparticles were immobilized to the natural nanofiber of scaffolds, they were able to load significantly more VEGF-169 (Figure 2a). We hypothesized that during the cross-linking procedure, electrovalent bonds turned into covalent bonds, which not only produces zero-length amide cross-linkages between the amido groups of nanoparticles and carboxyl groups of scaffolds, but also mediated the reaction between carboxyl groups of nanoparticles and amido groups of VEGF. This structure might confer to heparin/chitosan nanoparticles the capability to load more VEGF.

Currently, local delivery of angiogenic growth factors is the primary strategy used to promote vascularization within scaffolds. The established approaches include the encapsulation of growth factors in scaffolds and immobilization of growth factors to the surface of scaffolds by direct chemical cross-link.[16] These strategies could maintain a steady supplement of growth factors locally due to a delayed release from the decellularized scaffolds, which effectively induces angiogenesis within the engineered tissues. However, the drawbacks of the denaturation of growth factors due to residual cross-linkers, and complications in the host caused by systemic administration of nanoparticles, still hampered the clinical application of these engineered scaffolds. A significant advantage of our delivery system is that the nanoparticles and EDC modification mediated local delivery and controlled release of VEGF. In addition, with EDC modification, the initial burst of VEGF released was significantly reduced, which not only extended VEGF clearance time, but also reduced the toxicity of VEGF due to rapid release. The release pattern observed in this study suggests that 3 possible populations of VEGF-molecules might exist. The first population is the VEGF that was adsorbed to scaffolds and glycosaminoglycans, a component of extracellular matrix. This includes a nonspecific adsorption through electrostatic adherence and hydrophobic effects depending on the extracellular matrix in scaffolds. Although the physical adsorption of growth factors on the surface of scaffolds could also be achieved by heparin and fibronectin modification on the collagen scaffold and could effectively promote cell proliferation in vitro, it is less efficient in vivo.[40] The second population might be the major population. In this population, VEGF was sequence-specifically bound to heparin. The third

population is the VEGF covalently bonded to heparin by EDC modification. We proposed that EDC modification contributed to the controlled release of VEGF. In contrast, without EDC modification, most VEGF was immobilized to SF-NP via electrovalent bond to chondroitin sulfate, the main constituents of glycosaminoglycans.

The recruitment of functional cells such as endothelial and fibroblast cells plays a vital role in regeneration, while the extracellular matrix could sustain the growth and reproduction of the cells. Our in vitro study demonstrated that nanoparticle-localized VEGF led to endothelial cell proliferation in the scaffolds (Figure 3). Our in vivo study clearly demonstrated that massive new capillary formation (Figures 4, 5, and 6) was observed in the implanted scaffolds immobilized with nanoparticle-localized VEGF. However, a significant problem with VEGF alone is that it induces the formation of atypical blood vessels. These large, leaky vessels are not fully functional. Therefore, the addition of other stabilizing factors is necessary to induce the formation of more functional vessels. Importantly, implantation of scaffolds with nanoparticle-localized VEGF not only enhanced large vessel growth (Figure 4), but most of the vessels are small capillaries (Figures 5 and 6). The significant role of SF-NP-VEGF might be associated with either the localization of VEGF to the scaffold or the biological activity of heparin, because VEGF usually has diffusion limitations and fails to be actively taken up by cells residing on the peripheral surfaces of the scaffold. In addition, heparin could prevent early degradation of growth factors, while chitosan could stimulate cell attachment and growth.[26,28] Moreover, heparin is an effective anticoagulant used during vascular injury.[41]

We also observed massive cellular infiltration in the SF-NP-VEGF implants (Figure 5). The infiltrating cells were further verified to be mainly fibroblasts (Figure 7). This fibroblast infiltration was accompanied by significant synthesis of new collagen fibers (Figure 9) and glycosaminoglycans (Figure 10). Fibroblasts may synthesize collagen and other extracellular matrix proteins for further tissue remolding. This provided solid evidence for regeneration. Another significant advantage is that our system is highly biocompatible and biodegradable. For instance, the acellular scaffolds could provide plenty of highly homologous extracellular matrices to humans. Chitosan is a natural biocompatible and biodegradable cationic polysaccharide.[26] Heparin is a natural, linear polysaccharide present in many living organisms.[28] With physical self-assembly, the chitosan/heparin nanoparticles retained biological activities. Also, the whole system is composed of biomaterials without any artificial or synthetic materials. The highly biocompatible characteristic of the nanoparticles was shown by the limited macrophage repopulation observed in the early implantation stage (Figure 8). Macrophages are important contributors to biological scaffold degradation and early remodeling events.

Most current strategies for revascularization of scaffolds utilize growth factors to attract and localize vascular endothelial cells, such as the strategy described in this study. Most recently, a study with endothelial progenitor cells (EPC) demonstrated that EPC cultured in contact with heparinized matrices loaded with VEGF revealed the highest rate of cell proliferation.[42] Implantation of scaffolds seeded with VEGF-expressing stem cells led to a 2- to 4-fold increase in vessel density 8 weeks after implantation.[43] Attracting and localizing EPC could be a novel strategy for endothelialization because EPCs are the type of predifferentiated stem cells that have the potential to proliferate and differentiate into mature endothelial cells. Also, EPCs exhibited an excellent ability to enhance the function of ischemic organs by stimulating the re-endothelialization of injured blood vessels and by inducing and modulating vasculogenesis and angiogenesis in areas with reduced oxygen supply.[44,45] However, peripheral blood of healthy adults contains very low concentrations of EPCs. With our decellularized tissue-engineered scaffolds immobilized with nanoparticles localizing high loading of VEGF, EPCs might be effectively attracted and then endothelialized in vivo.

Conclusions

Besides the major finding that a controlled release of VEGF can enhance regeneration of decellularized BJV scaffolds, this system provided excellent biocompatibility. The functional heparin/chitosan nanoparticles exhibit high loading capacities, while EDC modification can mediate a controlled release of VEGF locally. Our results support heparin/chitosan nanoparticle as a functional drug delivery agent to localize VEGF onto scaffolds and keep its bioactivity stable for weeks. With accelerated regeneration and excellent biocompatibility, our system exhibited good therapeutic potential. Further studies with a longer follow-up period, a combination of multiple growth factors, and reconstruction of connections between pulmonary arteries and right ventricles of large animals should be conducted before this system can be applied in the clinic.

Acknowledgment

This project is financially supported by National "863" Program (2007 AA071900) and National Natural Science Foundation of China (81071275).

Disclosure

The authors declare no conflicts of interest.

References

1. Gui L, Muto A, Chan SA, Breuer CK, Niklason LE. Development of decellularized human umbilical arteries as small-diameter vascular grafts. *Tissue Eng Part A*. 2009;15(9):2665–2676.
2. Kaushal S, Amiel GE, Guleserian KJ, et al. Functional small-diameter neovessels created using endothelial progenitor cells expanded ex vivo. *Nat Med*. 2001;7(9):1035–1040.
3. Morritt AN, Bortolotto SK, Dilley RJ, et al. Cardiac tissue engineering in an in vivo vascularized chamber. *Circulation*. 2007;115(3):353–360.
4. Shen YH, Shoichet MS, Radisic M. Vascular endothelial growth factor immobilized in collagen scaffold promotes penetration and proliferation of endothelial cells. *Acta Biomater*. 2008;4(3):477–489.
5. Lu WD, Yu FL, Wu ZS. Superior vena cava reconstruction using bovine jugular vein conduit. *Eur J Cardiothorac Surg*. 2007;32(5):816–817.
6. Lu WD, Zhang M, Wu ZS, Hu TH. Decellularized and photooxidatively crosslinked bovine jugular veins as potential tissue engineering scaffolds. *Interact Cardiovasc Thorac Surg*. 2009:8:301–305.
7. Lu WD, Zhang M, Wu ZS, et al. The performance of photooxidatively crosslinked acellular bovine jugular vein conduits in the reconstruction of connections between pulmonary arteries and right ventricles. *Biomaterials*. 2010;31(10):2934–2943.
8. Park CJ, Clark SG, Lichtensteiger CA, Jamison RD, Johnson AJ. Accelerated wound closure of pressure ulcers in aged mice by chitosan scaffolds with and without bFGF. *Acta Biomater*. 2009;5(6):1926–1936.
9. Huang M, Vitharana SN, Peek LJ, Coop T, Berkland C. Polyelectrolyte complexes stabilize and controllably release vascular endothelial growth factor. *Biomacromolecules*. 2007;8(5):1607–1614.
10. Chung YI, Kim SK, Lee YK, et al. Efficient revascularization by VEGF administration via heparin-functionalized nanoparticle-fibrin complex. *J Control Release*. 2010;143(3):282–289.
11. Joung YK, Bae JW, Park KD. Controlled release of heparin-binding growth factors using heparin-containing particulate systems for tissue regeneration. *Expert Opin Drug Deliv*. 2008;5(11):1173–1184.
12. Ferrara N, Houck KA, Jakeman LB, Winer J, Leung DW. The vascular endothelial growth factor family of polypeptides. *J Cell Biochem*. 1991;47(3):211–218.
13. Steffens GC, Yao C, Prével P, et al. Modulation of angiogenic potential of collagen matrices by covalent incorporation of heparin and loading with vascular endothelial growth factor. *Tissue Eng*. 2004;10(9–10):1502–1509.
14. Yao C, Roderfeld M, Rath T, Roeb E, Bernhagen J, Steffens G. The impact of proteinase-induced matrix degradation on the release of VEGF from heparinized collagen matrices. *Biomaterials*. 2006;27(8):1608–1616.
15. Yao C, Markowicz M, Pallua N, Noah EM, Steffens G. The effect of cross-linking of collagen matrices on their angiogenic capability. *Biomaterials*. 2008;29(1):66–74.
16. Chiu LL, Radisic M. Scaffolds with covalently immobilized VEGF and Angiopoietin-1 for vascularization of engineered tissues. *Biomaterials*. 2010;31(2):226–241.
17. Rocha FG, Sundback CA, Krebs NJ, et al. The effect of sustained delivery of vascular endothelial growth factor on angiogenesis in tissue-engineered intestine. *Biomaterials*. 2008;29(19):2884–2890.
18. Nillesen ST, Geutjes PJ, Wismans R, Schalkwijk J, Daamen WF, van Kuppevelt TH. Increased angiogenesis and blood vessel maturation in acellular collagen-heparin scaffolds containing both FGF2 and VEGF. *Biomaterials*. 2007;28(6):1123–1131.
19. Wissink MJ, Beernink R, Pieper JS, et al. Immobilization of heparin to EDC/NHS-crosslinked collagen. Characterization and in vitro evaluation. *Biomaterials*. 2001;22(2):151–163.
20. Wissink MJ, Beernink R, Scharenborg NM, et al. Endothelial cell seeding of (heparinized) collagen matrices: effects of bFGF pre-loading on proliferation (after low density seeding) and pro-coagulant factors. *J Control Release*. 2000;67(2):141–155.
21. Hiemstra C, Zhong Z, van Steenbergen MJ, Hennink WE, Feijen J. Release of model proteins and basic fibroblast growth factor from in situ forming degradable dextran hydrogels. *J Control Release*. 2007;122(1):71–78.
22. Jay SM, Saltzman WM. Controlled delivery of VEGF via modulation of alginate microparticle ionic crosslinking. *J Control Release*. 2009; 134(1):26–34.
23. Pieper JS, Hafmans T, Veerkamp JH, van Kuppevelt TH. Development of tailor-made collagen-glycosaminoglycan matrices: EDC/NHS crosslinking, and ultrastructural aspects. *Biomaterials*. 2000;21(6):581–593.
24. Cai S, Liu Y, Zheng Shu X, Prestwich GD. Injectable glycosaminoglycan hydrogels for controlled release of human basic fibroblast growth factor. *Biomaterials*. 2005;26(30):6054–6067.
25. Zhong Y, Zhang L, Ding AG, et al. Rescue of SCID murine ischemic hindlimbs with pH-modified rhbFGF/poly(DL-lactic-co-glycolic acid) implants. *J Control Release*. 2007;122(3):331–337.
26. Kujawa P, Schmauch G, Viitala T, Badia A, Winnik FM. Construction of viscoelastic biocompatible films via the layer-by-layer assembly of hyaluronan and phosphorylcholine-modified chitosan. *Biomacromolecules*. 2007;8(10):3169–3176.
27. Zhu Y, Gao C, Liu X, He T, Shen J. Immobilization of biomacromolecules onto aminolyzed poly(L-lactic acid) toward acceleration of endothelium regeneration. *Tissue Eng*. 2004;10(1–2):53–61.
28. Liu Z, Jiao Y, Liu F, Zhang Z. Heparin/chitosan nanoparticle carriers prepared by polyelectrolyte complexation. *J Biomed Mater Res A*. 2007;83(3):806–812.
29. Sallustio F, Di Legge S, Marziali S, Ippoliti A, Stanzione P. Floating carotid thrombus treated by intravenous heparin and endarterectomy. *J Vasc Surg*. 2011;53(2):489–491.
30. Maegdefessel L, Linde T, Krapiec F, et al. In vitro comparison of dabigatran, unfractionated heparin, and low-molecular-weight heparin in preventing thrombus formation on mechanical heart valves. *Thromb Res*. 2010;126(3):e196–e200.
31. Schlitt A, Rupprecht HJ, Reindl I, et al. In-vitro comparison of fondaparinux, unfractionated heparin, and enoxaparin in preventing cardiac catheter-associated thrombus. *Coron Artery Dis*. 2008; 19(4):279–284.
32. Mao S, Shuai X, Unger F, Simon M, Bi D, Kissel T. The depolymerization of chitosan: effects on physicochemical and biological properties. *Int J Pharm*. 2004;281(1–2):45–54.
33. Meng S, Liu Z, Shen L, et al. The effect of a layer-by-layer chitosan-heparin coating on the endothelialization and coagulation properties of a coronary stent system. *Biomaterials*. 2009;30(12):2276–2283.
34. Rawlins JM, Lam WL, Karoo RO, Naylor IL, Sharpe DT. Quantifying collagen type in mature burn scars: a novel approach using histology and digital image analysis. *J Burn Care Res*. 2006;27(1):60–65.
35. Scott JE. Amplification of staining by Alcian Blue and similar ingrain dyes. *J Histochem Cytochem*. 1972;20(9):750–752.
36. Knoess M, Krukemeyer MG, Kriegsmann J, Thabe H, Otto M, Krenn V. Colocalization of C4d deposits/CD68+ macrophages in rheumatoid nodule and granuloma annulare: immunohistochemical evidence of a complement-mediated mechanism in fibrinoid necrosis. *Pathol Res Pract*. 2008;204(6):373–378.
37. Kopecky M, Semecky V, Nachtigal P. Vimentin expression during altered spermatogenesis in rats. *Acta Histochem*. 2005;107(4):279–289.
38. Hu Y, Jiang X, Ding Y, Ge H, Yuan Y, Yang C. Synthesis and characterization of chitosan-poly(acrylic acid) nanoparticles. *Biomaterials*. 2002;23(15):3193–3201.
39. Chen MC, Wong HS, Lin KJ, et al. The characteristics, biodistribution and bioavailability of a chitosan-based nanoparticulate system for the oral delivery of heparin. *Biomaterials*. 2009;30(34):6629–6637.
40. Visser LC, Arnoczky SP, Caballero O, Kern A, Ratcliffe A, Gardner KL. Growth factor-rich plasma increases tendon cell proliferation and matrix synthesis on a synthetic scaffold: an in vitro study. *Tissue Eng Part A*. 2010;16(3):1021–1029.
41. Yang XB, Bhatnagar RS, Li S, Oreffo RO. Biomimetic collagen scaffolds for human bone cell growth and differentiation. *Tissue Eng*. 2004;10(7–8):1148–1159.

42. Grieb G, Groger A, Piatkowski A, Markowicz M, Steffens GC, Pallua N. Tissue substitutes with improved angiogenic capabilities: an in vitro investigation with endothelial cells and endothelial progenitor cells. *Cells Tissues Organs*. 2010;191(2):96–104.
43. Yang F, Cho SW, Son SM, et al. Genetic engineering of human stem cells for enhanced angiogenesis using biodegradable polymeric nanoparticles. *Proc Natl Acad Sci U S A*. 2010;107(8):3317–3322.
44. Hung HS, Shyu WC, Tsai CH, Hsu SH, Lin SZ. Transplantation of endothelial progenitor cells as therapeutics for cardiovascular diseases. *Cell Transplant*. 2009;18(9):1003–1012.
45. Kirton JP, Xu Q. Endothelial precursors in vascular repair. *Microvasc Res*. 2010;79(3):193–199.